4^{th} URSI AT-RASC, Gran Canaria, 19 – 24 May 2024

Measurements of the Time-Variant Indoor Radio Channel in the D-Band at 160 GHz for Communication and Sensing

Wilhelm Keusgen*(1) and Taro Eichler(2)
(1) Technische Universtität Berlin, Berlin, Germany
(2) Rohde & Schwarz, München, Germany

Abstract

This paper introduces a measurement setup and an evaluation method for the characterization of the mobile radio channel in the D-Band. The 2-dimensional system functions in delay / frequency and time / Doppler frequency domain and the corresponding 1-dimensional power profiles and spectra were derived and demonstrated with exemplary indoor measurements. The proposed method is valuable for 6G communication and sensing applications in particular.

1 Introduction

The measurement and the modeling of the wireless radio channel is crucial for design and optimization of wireless communication systems as well as for sensing and radar applications. With the current trend to much higher carrier frequencies up to 300 GHz and much larger transmission bandwidths of several GHz, as it is for example envisioned for the sixth generation of mobile communication systems, this task becomes more challenging. Current state-of-the art channel models cover just the frequency range up to 100 GHz [1] and thus there is a large interest in conducting channel measurements and creating channel models - both for communication and sensing. So far, the measurements focus on the observations of static channels - mainly due to restrictions in the measurement hardware (channel-sounder) and even the established channel models [1] do not rely on a solid base of mobile or time-variant measurements for its upper frequency range. In this paper, we introduce first exemplary results for measurement of the time varying indoor radio channel in D-Band (110 GHz - 170 GHz), which expand channel observations in this frequency band to the time and Doppler frequency domain for the first time.

2 The System Functions

The description of the time-variant or mobile radio channel by means of four 2-dimensional (2-D) complex valued system functions was introduced by Bello [3] (see Fig. 1). These system functions are defined with respect to two sets of conjugate variables or Fourier pairs (connected by the $\circ\!\!-\!\!\bullet$ symbol): frequency f and delay τ as well as time t and Doppler frequency ν. Assuming the channel being a linear but time-variant system, such a system could be naturally described by means of a time-variant channel impulse response - known as Input Delay spread $h(t,\tau)$ or a time-variant transfer function - known as Time-Variant Transfer Function $T(t,f)$, which are both related by Fourier transforms in the delay - frequency dimension. The Fourier transform of $h(t,\tau)$ in the time - Doppler frequency domain leads to the Doppler-Delay Spread $S(\nu,\tau)$. The additional Fourier-Transformation of $S(\nu,\tau)$ with respect to τ results in the Output Doppler-Spread $H(\nu,f)$, which could also be derived by Fourier transform of $T(t,f)$ in the time - Doppler frequency domain as illustrated by the transformation symbols in Fig. 1. Assuming a frequency-selective radio channel with multiple propagation paths, $T(t,f)$ shows the highest variation of all system functions, due to the joint effect of small scale fading and time-variance, whereas $h(t,\tau)$ and $H(\nu,f)$ show variation in one dimension only and $S(\nu,\tau)$ being the most stable representation. This stability is directly related to the magnitude of the system functions being localized in prominent peaks (highest stability, as in $S(\nu,t)$), within discrete lines for $h(t,\tau)$, and $H(\nu,f)$) or showing no localization at all (lowest stability, as in $T(t,f)$).

We derive a a set of real valued 1-dimensional (1-D) power profiles or power spectra from the 2-D system functions by power summation – denoted by $\sum P$ – or by power averaging – denoted by $\bar{P}$ – across one respective dimension of the system function, whereas the power is calculated from the squares of the complex magnitudes (see Fig. 1). Thus, the well known Power-Delay Profile $p_d(\tau)$ (see e.g [2]) gives the expected power over τ and can be calculated from $h(t,\tau)$ by averaging across time t or by summation over Doppler-frequency ν in $S(\nu,\tau)$. In addition to $p_d(\tau)$, here we define also the further 1-D power functions: Power Time Profile $p_t(t)$, the Doppler Power Spectrum $S_D(\nu)$, and the Power Spectrum $S_f(f)$. These power functions might give a better insight on the properties of time-variant fading channels, especially $p_t(t)$ and $S_D(\nu)$, which do not include an averaging over time.

Furthermore, the repeated application of power summation

The authors acknowledge the financial support by the German Federal Ministry of Education and Research within the joint project 6G-RIC, project identification number: 16KISK020K.

of $p_d(\tau)$ and $S_D(\nu)$ as well as the power averaging of $p_t(t)$ and $S_f(f)$ will result in the overall mean received power or the mean channel gain for the observed channel.

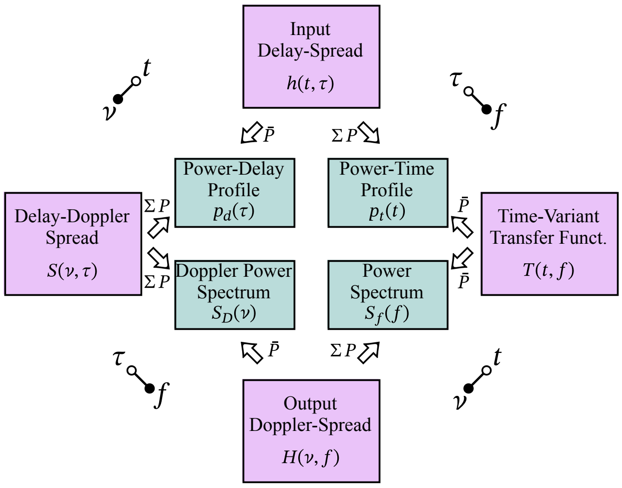

Figure 1. The set of 2-dimensional system functions and the corresponding 1-dimensional power functions.

3 Measurement Setup

The broadband measurement of the time-variant sub-THz radio channel was performed using a fast time-domain channel sounder, on the basis of commercial test and measurement equipment, operating in the D-Band (110 GHz - 170 GHz). Here, "time domain" refers to a measurement method, exciting the channel with broadband periodic signals and measuring the channel completely during one signal period, compared to the "frequency domain" measurement method, probing one frequency point of the channel transfer function after the other using continuous wave signals – usually utilizing a vector network analyzer. Historically, the time-domain method embodies direct correlation, yielding channel impulse responses $h(t,\tau)$, but it is implemented fully digitally here. Since this approach is much more flexible and allows for short measurement duration, which means a higher temporal sampling of the time variant channel, this method is chosen here. With this model, there is always a trade-off between measurement speed i.e the maximum resolvable Doppler frequency (short measurement duration) and the sensitivity i.e. dynamic range (increases with long measurement duration) possible. Additionally, the lower theoretical limit of the measurement duration is the maximum access delay, which is not a concern for most realistic scenarios.

At the transmitter side (TX) a vector signal generator (R&S®SMW200A with external frequency extender R&S®FE170ST), transmitting a periodic Frank-Zadoff-Chu correlation sequence [4] with 2 GHz bandwidth and 250 μs length. A signal analyzer (R&S®FSW with frequency extender R&S®FE170SR) was used on the receiver side (RX) to sample and store the received signals. Synchonization of both sides and triggering of the receiver was implemented using two cables, whereas untethered operation is also possible using specific synchronisation devices. The setup was controlled by a host-PC. The measured base-band signals are calibrated in frequency domain with a back-to-back reference measurement (using a calibrated attenuator) yielding directly the Time-Variant Transfer Function $H(t,f)$. The estimation of $H(t,f)$ and the further data processing was done offline in MatLab®. Table 1 summarizes the technical parameters of the used setup, which correspond to or exceed the current state of the art.

Table 1. Parameters of the channel sounder

Parameter	Value and unit
Carrier Frequency	160 GHz
Measurement bandwidth	2 GHz
Sequence length (samples / time)	500,000 / 250µs
Number of sequences	3200
Measurement time	800 ms
Temporal resolution	0.5 ns
Delay resolution	250 µs
Doppler resolution	1.25 Hz
Frequency resolution	4 kHz
Maximum Doppler frequency	2 kHz
Maximum speed of receiver	3.6 m/s
Maximum speed of reflector	1.8 m/s
Maximum access delay	250 µs
Processing gain	57.0 dB
Transmit power	4.5 dBm
Noise floor	-125 dB

4 Data Processing

The output of the channel-sounder is the Time-Variant Transfer Function $T(t,f)$ sampled on a discrete time-frequency grid. Thus, the other system functions ($h(t,\tau)$, $S(\nu,\tau)$, and $H(\nu,f)$) can be calculated by means of discrete Fourier transforms. Since the measurements were hard limited in time t (by observation time) and frequency f (by observation bandwidth), the conjugate dimensions (ν and τ) are strongly affected by sidelobes, which could be suppressed by an appropriate window taper function applied in the time or in the frequency domain. The authors propose the use of ultraspherical windows [5], which give full control of the sidelobe levels and its shape. Here, the minimum sidelobe suppression was chosen to 70 dB according to the observed dynamic range and a sidelobe taper parameter of 1, which gives a slight decrease of the sidelobes. Since the sequence length is much larger as the observable maximum excess delay or $\tau_{\max}$ it could also be useful to apply a window in the delay domain which suppresses all values beyond $\tau_{\max}$ and thus reduces the noise in the conjugate domain i.e. the frequency domain. In practice, measurements with low dynamic range and high path-loss, $T(t,F)$ and $S_f(f)$ could not be observed, without this type of noise removal. The same applies for the Doppler-frequency domain in a scenario with a limitation of the maximum Doppler-frequency to $|\nu_{\max}|$. A windowing could suppress noise in the time domain and for the corresponding Power Delay Profile $p_d(\tau)$. For this type of noise-removal a flat-top window like a Tuckey window (cosine-tapered window) is suggested. When applying the mentioned windows in the four domains, a proper normalization, depending on the magnitude or the energy of the pulse is required. Furthermore, an interpolation or oversampling in the delay or in the Doppler-frequency domain could be performed, to allow for a better observation of peaks, especially for the 1D functions Power-Delay Profile ($p_d(\tau)$) and Doppler Power spectrum ($S_D(\nu)$). The interpolation can be easily implemented by zero-padding in the conjugate domains.

5 Experimental Measurements

A measurement campaign in a typical conference room scenario was conducted to test the measurement setup and the proposed evaluation method. The room had a size of approx 8m $\times$ 8m and was equipped with tables and chairs. Two typical situations were tested: a bi-static scenario with separated transmitter and receiver as is common for a wireless communication situation and a mono-static scenario with transmitter and receiver at the same place as is typical for a radar or sensing application. Two different antennas – vertical polarized open waveguide with 10.5 dBi gain, and vertical polarized waveguide horn with 20 dBi gain – were used. In the bi-static scenario the link distance was 3.8 m, with the antennas being aligned. In the mono-static scenario, both antennas were directed towards an opposite wall in 5.1 m distance, which was highly reflective due to a metallic whiteboard. Both scenarios were measured including longitudinal and transverse movements of a person.

6 Results

Fig. 2 shows $T(t,f)$ as the direct output of the channel-sounder for a bi-static communication type measurement with open waveguide antennas on both sides and a person crossing the link perpendicular in the middle of the link distance. One can clearly see the drop in power, caused by the blockage, as well as a moderate frequency selectivity, related to multipath propagation. The blockage effect can be well observed in the Power Time Profile (Fig. 3). Fig. 4 and Fig. 5 show the Input Delay Spread and the Power Time Profile when using horn antennas on both sides and the person is crossing the link close to the TX antenna. One can recognize the stronger attenuation of almost 30 dB of the blocking event, as well as the multiple echos from the rectangular room in the Input Delay Spread Function. The characteristic shape of the Power Time Profile corresponds very well to the observations in the microwave range in [6] and its modeling with the double knife edge and could be subject to further investigations. Fig. 6 and Fig. 7 show $h(t,\tau)$ and $p_d(\tau)$ for a mono-static scenario using 20 dBi antennas and a person crossing the direct link in the middle between TX and Rx and the opposite wall. The figures

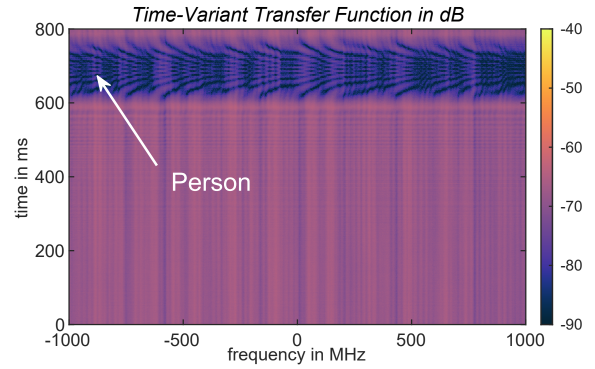

Figure 2. Time-Variant Transfer Function for 10.5 dBi antennas and blockage by a person in the middle of the link

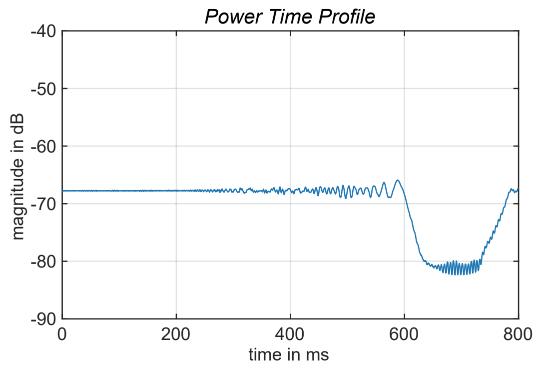

Figure 3. Power Time Profile for blockage by a person in the middle of the link

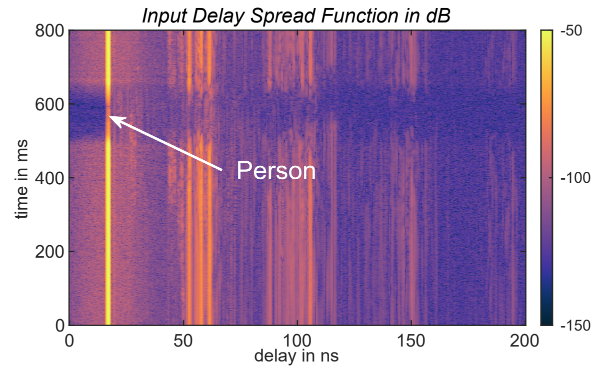

Figure 4. Input Delay Spread Function for 20 dBi antennas and blockage by a person close to TX

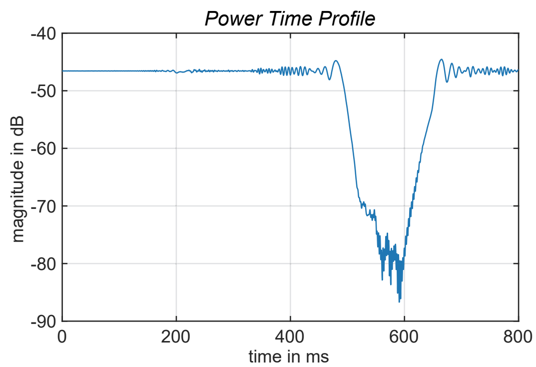

Figure 5. Power Time Profile for blockage close to TX

shows clearly the multipath channel with the strongest reflection at around 30 ns corresponding to the echo from the opposite wall in 5.1 m distance. At around 600 ms the person blocks the path to the wall and creates a new echo at around 10 ns delay. Although the person walks perpendicular to the main path, it creates some weak and mainly positive Doppler frequencies, which can be seen in the Output Doppler Spread Function in Fig. 8 and also in the Doppler Power Spectrum (not shown). A stronger Doppler effect is expected, if the person moves transverse to the main path. Fig. 9 and 10 show the corresponding Delay Doppler Spread and Doppler Power Spectrum for this case (using 10.5 dBi antennas).

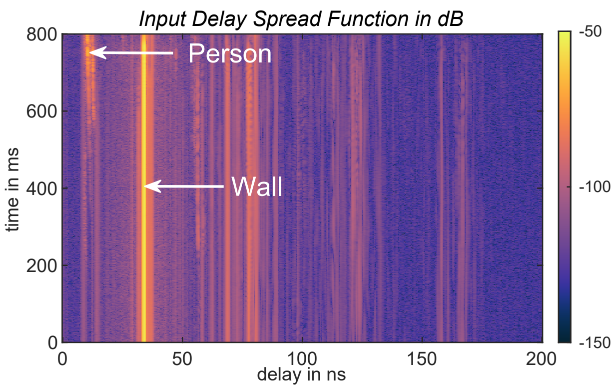

Figure 6. Input Delay Spread, 20 dBi, crossing

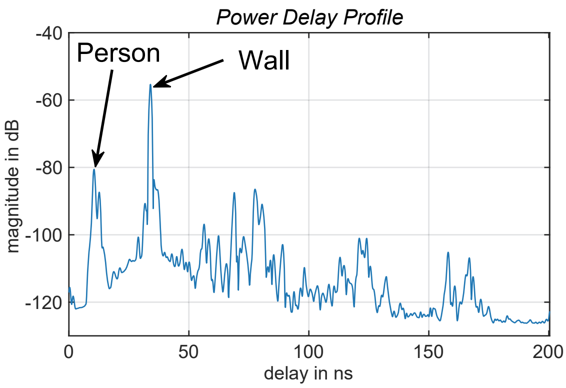

Figure 7. Power Delay Profile, 20 dBi, crossing

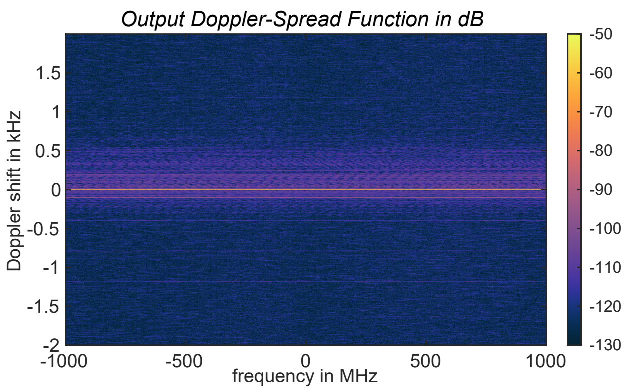

Figure 8. Output Doppler Spread, 20 dBi, crossing

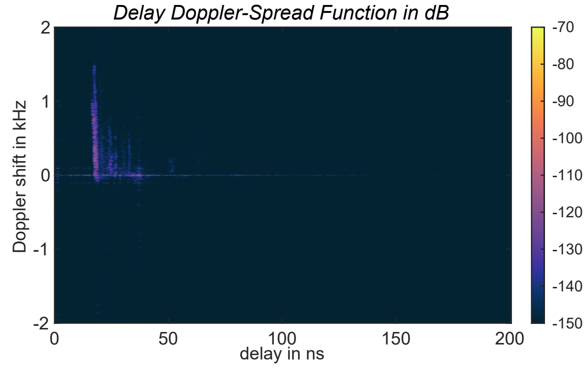

Figure 9. Delay Doppler Spread, 10.5 dBi, approaching

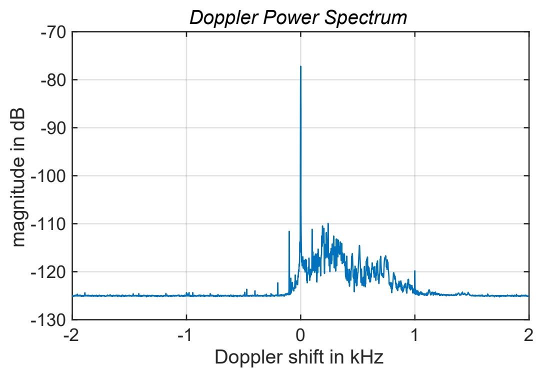

Figure 10. Doppler Power Spect., 10.5 dBi, approaching

References

[1] ETSI TR 138 901 "5G; Study on channel model for frequencies from 0.5 to 100 GHz", 3GPP TR 38.901 version 16.1.0 Release 16, https://www.etsi.org.

[2] "Mobile Radio Communications," 2nd Edition, Raymond Steele (Editor), Lajos Hanzo (Editor) ISBN: 978-0-471-97806-0 May 1999 Wiley-IEEE Press.

[3] P. Bello, "Characterization of Randomly Time-Variant Linear Channels," in *IEEE Transactions on Communications Systems*, vol. 11, no. 4, pp. 360-393, December 1963, doi: 10.1109/TCOM.1963.1088793.

[4] D. Chu, "Polyphase codes with good periodic correlation properties (Corresp.)," in *IEEE Transactions on Information Theory*, vol. 18, no. 4, pp. 531-532, July 1972, doi: 10.1109/TIT.1972.1054840.

[5] S.W. Bergen, A. Antoniou, "Design of Ultraspherical Window Functions with Prescribed Spectral Characteristics", *EURASIP J. Adv. Signal Process.* 2004, 196503 (2004). https://doi.org/10.1155/S1110865704403114.

[6] J. Kunisch and J. Pamp, "Ultra-wideband double vertical knife-edge model for obstruction of a ray by a person," *2008 IEEE International Conference on Ultra-Wideband*, Hannover, Germany, 2008, pp. 17-20, doi: 10.1109/ICUWB.2008.4653341.